NASA TECHNICAL NOTE

NASA TN D-7700

NASA TN D-7700

DYNAMIC-SCANNING-ELECTRON-MICROSCOPE STUDY OF FRICTION AND WEAR

by William A. Brainard and Donald H. Buckley

Lewis Research Center
Cleveland, Ohio 44135

NATIONAL AERONAUTICS AND SPACE ADMINISTRATION • WASHINGTON, D. C. • JUNE 1974

1. Report No.	2. Government Accession No.	3. Recipient's Catalog No.
NASA TN D-7700		

4. Title and Subtitle	5. Report Date
DYNAMIC-SCANNING-ELECTRON-MICROSCOPE STUDY OF FRICTION AND WEAR	JUNE 1974
	6. Performing Organization Code

7. Author(s)	8. Performing Organization Report No.
William A. Brainard and Donald H. Buckley	E-7913
	10. Work Unit No. 502-01

9. Performing Organization Name and Address	11. Contract or Grant No.
Lewis Research Center National Aeronautics and Space Administration Cleveland, Ohio 44135	
	13. Type of Report and Period Covered
12. Sponsoring Agency Name and Address	Technical Note
National Aeronautics and Space Administration Washington D.C. 20546	14. Sponsoring Agency Code

15. Supplementary Notes

16. Abstract

A friction and wear apparatus was built into a real time scanning electron microscope (SEM). The apparatus and SEM comprise a system which provides the capability of performing dynamic friction and wear experiments in situ. When the system is used in conjunction with dispersive X-ray analysis, a wide range of information on the wearing process can be obtained. The type of wear and variation with speed, load, and time can be investigated. The source, size, and distribution of wear particles can be determined and metallic transferal observed. Some typical results obtained with aluminum, copper, and iron specimens are given.

17. Key Words (Suggested by Author(s))

Friction
Wear
Scanning electron microscope

18. Distribution Statement

Unclassified - unlimited
Category 15

19. Security Classif. (of this report)	20. Security Classif. (of this page)
Unclassified	Unclassified

* For sale by the National Technical Information Service, Springfield, Virginia 22151

DYNAMIC-SCANNING-ELECTRON-MICROSCOPE STUDY OF FRICTION AND WEAR

by William A. Brainard and Donald H. Buckley

Lewis Research Center

SUMMARY

A specially constructed friction and wear apparatus was built into a real time scanning electron microscope (SEM) to provide for dynamic observation of the friction and wear process. The friction apparatus employs a small 0.1 centimeter-diameter rider which slides against a flat rotating disk. The SEM and friction and wear apparatus comprise a system which enables the wearing process to be studied in great detail over a range of magnifications and depth of focus. The system provides for a wide range of loading and speed as well as optimal viewing conditions. The wear process can be studied by viewing the prow, the wake or side of the rider-disk interface. Very precise control of the point of rider-disk contact permits any area of interest to be examined at increasing magnifications.

A series of experiments with aluminum, copper, and iron specimens were performed to determine the type of information that can be gained with such a system. When the system is used in conjunction with a dispersive X-ray analyzer, a wide variety of information can be gained. A continuous dynamic correlation between friction and the physical interactions of the sliding surfaces as well as the type of wear occurring and the variation in wear with speed, load, and time can be investigated. The source, size, and distribution of wear particles can be determined and metallic transfer can be observed.

INTRODUCTION

The study of the friction, adhesion, and wear process has increasingly utilized improved analytic tools and techniques. The friction and wear process is now routinely studied with modern equipment such as low energy electron diffraction (LEED), Auger emission spectroscopy (AES), and field ion microscopy (FIM) (ref. 1). In addition to analyzing the surface from either a chemical or structural viewpoint, it is often desirable

to actually visualize the wear process.

In regard to visualization, many investigators have found the scanning electron microscope (SEM) extremely useful for post-testing analysis (ref. 2 and 3). The friction and wear process is, however, a dynamic one and post-testing viewing is not completely satisfactory in the sense that it is difficult to relate a dynamic process to static observations.

The usefulness of studies in which the friction experiment was actually conducted in situ in the SEM has been demonstrated by Skinner, Gane, and Tabor (ref. 4).

The authors of reference 4 constructed a micro-friction and wear apparatus which was incorporated into the specimen stage of the SEM. Their system was, however, not truly dynamic because it did not provide for real time viewing because of apparent instrumental limitations (i.e., slow electron beam scanning).

With the improvement in commercial SEM's real time scanning is readily achievable by means of a closed circuit television system that provides for several frames per second.

The objective of this report is to present the application of real time scanning electron microscopy to the study of friction and wear. Some preliminary data to describe the type of unique information that can be gained from such a system will be discussed. The materials that were used were aluminum, copper, and iron. These materials in combination provided a range of wearing conditions from relatively mild to severe. A series of experiments were run with like and unlike materials, with soft materials sliding on harder materials and with harder materials sliding on softer ones. These materials, while certainly not totally representative of all metal-metal friction combinations, do provide some of the more common wear situations.

APPARATUS

The friction and wear experiments were conducted in the vacuum chamber of the SEM. A commercial SEM was modified by the addition of the friction and wear apparatus which is shown in the photograph in figure 1. The SEM is a field emission electron source type which provides for real time viewing on a closed circuit television system at 15 complete frames per second.

The specimen chamber is mechanically fore pumped and ion pumped to a pressure of 10^{-6} to 10^{-7} torr at which pressure the experiments were conducted.

The friction and wear apparatus used for these experiments is shown schematically in figure 2. A disk specimen 1.9 centimeters in diameter is mounted on an adapter to the rotary specimen feedthrough. The surface of the disk is inclined at approximately 83° with respect to the electron beam. This steep angle permits the interface to be viewed from a near side view. A variable speed electric motor and gear train is attached to the

external rotary specimen feedthrough to provide rotation of the disk from 0.1 to 10 rpm. The rotation can either be clockwise or counterclockwise to provide for SEM observation of either the prow or wake of the rider disk contact. In addition, a side view of the wearing process can be observed, however, without the capability of friction force measurements.

The rider specimen is 0.1 centimeter in diameter with a 0.05 centimeter radius on the end. In addition, a 20^{o} taper was machined on the shank down to the radius in order to reduce the shadowing of the interface by the radius extending out beyond the actual contact point. The schematic of figure 2 shows the test specimen configuration.

The rider is mounted in an arm which can be moved in and out as well as up and down and laterally by means of a bellows and gimbal system. The gimbal system is comprised of a precision optical orientor which is mounted on a translational stage. This stage and the optical orientor are micrometer controlled thereby allowing very precise positioning of the rider on the disk under the scanning beam. The precision with which the rider can be positioned is demonstrated in figure 3. The rider specimen has been manipulated by the gimbal system while viewing the position on the SEM monitor into the slot of the number 1-64 screw which holds the disk specimen onto the rotating shaft.

The arm in which the rider is mounted contains two flex bands of beryllium-copper upon which strain gages are attached. One band, mounted parallel to the disk surface is used to measure the normal load applied to the contact. The other band and strain gage which are mounted perpendicular to the disk surface are used to monitor the friction force. In addition, another strain gage is mounted on the bottom of the loading beryllium-copper band and can be used to measure the force of adhesion between the rider and disk. The normal loading is accomplished by allowing the magnets which are mounted on the optical orientor ring to pull the arm downward to the disk surface.

The strain gage output of the load sensing gage is amplified and displayed on a digital millivolt meter which with suitable calibration provides for a direct reading of the load being applied. The friction force gage is read out either on a strip chart recorder or oscilloscope to provide for the observation of the friction trace which is more transient in nature.

The entire friction test is viewed on the television monitor of the SEM and the video signal is recorded along with audio comments on video tape to provide for data recording. The tape can be played back in slow motion and stop action to facilitate interpretation. In addition kinescopic motion pictures can readily be made from the video tape.

To provide for an analysis of the wear track, an energy despersive X-ray analyzer is mounted on the SEM. The analyzer has 400 channels and a resolution of 170 electron volts. Also provided is the capability of elemental mapping. The rider specimen, because of the geometry of the system, blocks the detection of those X-rays from the surface which are in the straight line defined by the rider and X-ray detector as shown in figure 4. The reciprocal image of the rider and disk shows those areas as dark shadows.

These shadow-like regions are the areas where generated X-rays are blocked from being detected by the rider specimen.

PROCEDURE

The rider and disk specimens were machined to shape by conventional techniques. Following machining, the specimens were polished by hand with metallurgical polishing papers and then cleaned with acetone in an ultrasonic cleaner. Following cleaning the specimens were mounted in the SEM specimen chamber, and the system evacuated to 10^{-6} to 10^{-7} torr. The SEM was turned on and the specimens manipulated until the rider contacted the disk at a point where with increasing magnification the contact was in view. The load was then applied by micrometer control to 50 grams. These loads produced Hertzian stresses in the contact zone ranging from 56.9 kg/mm^2 for aluminum on aluminum to 95.5 kg/mm^2 for copper on iron. Sliding was then initiated by turning on the electric drive motor and visual, audio, and friction data recorded.

Often it was necessary to reset the point of rider-disk contact because of the tendency of the friction force to pull the rider out of the field of view. This problem is particularly true of materials which exhibit pronounced stick-slip friction behavior. In these cases, the rider would be dragged out of view during the stick portion of the friction trace and come back into view during the slip portion of the trace.

Following running both the wear tracks and the rider specimens were examined with the despersive X-ray analyzer to determine if any metallic transfer took place. If transfer was observed, elemental X-ray maps were made to determine the distribution of the transferred material.

RESULTS AND DISCUSSION

Aluminum sliding on aluminum is representative of a soft metal sliding on itself. This combination exhibited pronounced stick-slip behavior and a high average friction coefficient of 0.82. During the stick portion, the rider was pulled backward by the friction force essentially increasing the radius of the point of contact slightly from the disk center. This caused the wear track generated to zig outward toward the circumference of the disk. When slip occurred, the rider-disk contact moved rapidly inward creating a zag toward the center of disk. The zig-zag character of the stick-slip track after several passes is shown clearly in figure 5. An enlarged view of the point of slip is also shown. A buildup of aluminum formed in front of the rider restrains the rider from sliding thus creating the stick condition.

When the spring force of the deflected beryllium-copper band exceeds the strength of the barrier, slip occurs and the rider slides past the side of the barrier shearing some of it off. With continued sliding, considerable aluminum wear debris accumulated on the rider forming an aluminum prow. Because this prow is in almost continuous contact with the rotating disk, it work hardens very rapidly. From table I, it can be seen that the

hardness of aluminum doubles with 20 percent cold work. Thus, the hardened prow acts like a cutting edge and serves to shear streamers of metal out of the softer disk. This is seen clearly in figure 6. Note that the origin of the metal curls is at the tip of the prow considerably in front of the rider. Some of the curls observed were as much as a centimeter long. The thickness was estimated to be approximately 10 micrometers. Once the shearing process began, friction remained steady until the termination of the curl.

Figures 7 and 8 present the disk wear track and rider wear scar for the aluminum rider sliding on iron along with X-ray maps of each of the worn surfaces. The significant feature observed on the iron track is the peeled up layers of iron similar to those observed for copper sliding on copper (ref. 3). This peeled up structure is believed to be caused by slip-band fracture brought about due to the stress imposed by compression of loading and the tensile stress of the adhesion between the rider and disk. As the rider slides, the adhered iron is peeled out of the surface with separation occurring along the fracture.

The friction initially was smooth at 0.45 but increased after several passes to 0.73 with some stick-slip behavior observed. X-ray maps taken after running shows metallic transfer had occurred to both rider and disk. Small discrete pieces of aluminum were observed on the disk wear track very randomly distributed. The rider showed iron on the wear scar distributed rather uniformly over the surface. Judging from the distribution of X-ray counts, the iron wear debris were small with no spot concentrations as might be observed with larger fragments. It appears as if these small wear fragments of iron were embedded in the much softer aluminum bulk.

Two-way transfer was also observed with aluminum sliding on copper (figs. 9 and 10). Again, severe wearing of the disk occurred. Severe stick-slip behavior was observed after several revolutions with the coefficient of friction increasing to an average of 0.78 and peaking during stick at 1.2. The first few revolutions were characterized by transfer of fragments of aluminum onto the copper surface. However, with increased sliding, the aluminum wear fragments collected on the rider forming a large prow. Severe wearing of the copper then began, primarily seeming to occur during the rapid slip portion of the frictional trace. The wear track appears to have an overall fractured appearance with very little evidence of plastic flow. The appearance is similar to that of a spall.

X-ray maps indicated that the aluminum transferred to the copper is again randomly distributed in discrete fragments which appear to be oriented by plastic flow parallel to the sliding direction. The copper transferred to the rider appears similar to the iron transfer being more uniform and not concentrated in larger fragments.

Figures 11 and 12 present micrographs taken for copper sliding on iron and iron sliding on copper, respectively. The friction coefficient in both cases was nearly the same (0.64 and 0.68, respectively); however, for copper sliding on iron, the friction

was smooth and constant during the run while when the couple was reversed, stick-slip occurred. The iron disk with copper as the rider was not damaged visibly; however, a dark contrast in the secondary electron image occurred in the track region which may have been due to an extremely thin transfer film of copper on the iron. X-ray analysis of the darkened track region did not show any copper; however, the film may have been too thin for detection. Various estimated put the escape depth of secondary electrons between 1×10^{-8} to 5×10^{-8} meters (100 and 500 Å) (ref. 5). Thus most of the X-rays produced will characterize below that region and not the true surface layers. If the contrast obtained on the iron wear track is due to a change in conductivity due to a copper transfer film, then the film is probably less than a few hundreths of a micrometer thick. The X-ray map of the copper rider showed the presence of iron in the wear region, with same characteristic uniform distribution as noted before.

With the couple reversed, no iron transfer onto the copper disk was observed. Significant wearing of the copper disk occurred however. Relatively large wear fragments of copper were generated and adhered to the iron rider. These fragments built up in the contact region so eventually the iron rider was lifted off the sliding surface by the debris and the sliding that occurred was that of the adhered copper debris sliding on the copper disk. This is shown clearly in figure 12(a) where the iron rider itself is not contacting the disk but rather is riding on the adhered debris. Although large wear fragments of copper were generated, no overt machining of the surface such as observed with aluminum sliding on aluminum was observed. No curls of copper were generated but rather the debris was the result of accumulation of thin copper lanellae.

For iron sliding on aluminum, two different wear behaviors were observed. When the iron rider was mounted in a manner that deflection of the beryllium-copper bands could occur, pronounced stick-slip behavior was observed and the aluminum wear track had a periodic fractured appearance as shown in figure 13(a). As with aluminum sliding on copper, this fracture occurred during the rapid slip portion of the friction trace. Note in the right side of the micrograph in 13(a), a stick-slip track ending in a fractured periodic track. When the rider specimen was mounted in a restrained manner, the wear was completely different. The wear track was generated by a cutting action as shown in figure 14. The machining of the aluminum was caused by the buildup of a work-hardened prow of transferred aluminum. The wear track had a smooth appearance as shown in figure 13(b). Figure 15 is a micrograph of the iron rider and the transferred aluminum prow taken after running in the restrained position. The fact that the type of wear is influenced by the testing mode is a serious consideration that must be evaluated further.

A system such as that employed herein can be utilized to study many other materials in addition to those discussed. Various material properties of metals and alloys such as grain boundary or phase concentrations effects on friction and wear can be evaluated. In addition, thin film lubrication with either metallic films such as lead or gold or inorganic

semiconductors such as MoS_2 can be studied. With proper care, certain polymers and plastic composite materials can be investigated with the friction-SEM system.

CONCLUDING REMARKS

The addition of a friction and wear apparatus to a scanning electron microscope with real time scanning provides for in situ experimentation and the ability to observe the friction and wear process at a very basic level. The system developed for this purpose provides the following:

1. Precise specimen positioning which is necessary for keeping the contact region in the field of view at increased magnifications.

2. A low-angle view relative to the disk surface of the actual sliding interface.

3. SEM viewing of the prow, the wake, or side of the rider-disk contact region with continuous friction measurements in prow or wake positions.

4. A loading system providing for continuous loading from 1 to 75 grams force.

5. A continuously variable speed control from 0.1 to 10 rpm, which depending on the radial distance of the contact from the disk center, provides surface sliding speeds from 0.94 to 0.003 centimeter per second.

6. Dynamic data recording of visual information on video tape.

Friction and wear tests conducted using several representative materials on this system have indicated that considerable information can readily be gained. When used in conjunction with a dispersive X-ray analyzer, the following types of information were observable:

1. The friction coefficient and the correlation of the variation with the actual wear process at any point in real time.

2. The type of wear such as adhesive or abrasive wear and changes in wear behavior with time, speed, or load.

3. Identification of the primary wearing surface and source of wear particles.

4. The size, shape, distribution, and agglomeration characteristics of the wear particles and their influence on the wearing process.

5. The observation of metallic transfer between the sliding surfaces.

The friction tests for the specific material combination showed the following:

1. The primary wear mechanism for aluminum sliding on aluminum was a shearing of the disk by a work hardened aluminum prow.

2. For iron sliding on aluminum, the aluminum wear debris collects on the iron slides forming a prow. After this occurs, the friction and wear behavior become identical to the aluminum on aluminum.

3. With aluminum on iron, aluminum on copper, and copper on iron two-way transfer was observed, that is, rider wear debris was observed by X-ray on the disk wear track and disk wear debris was observed on the rider in the contact region.

4. Copper sliding on iron showed the lowest friction and minimum wear to both surfaces. With the couple reversed (i.e., iron sliding on copper) severe wear occurs by the formation of a prow on the iron slider. The prow is formed by agglomeration of transferred copper.

Lewis Research Center,
National Aeronautics and Space Administration,
Cleveland, Ohio, March 22, 1974,
502-01.

REFERENCES

1. Ferrante, John; Buckley, Donald H.; Pepper, Stephen V.; and Brainard, William A.: Use of LEED, Auger Emission Spectroscopy and Field Ion Microscopy in Microstructural Studies. Microstructural Analysis: Tools and Techniques, J.L. McCall and William M. Mueller, eds., Plenum Publishing Corp. 1973, pp. 241-279.

2. Brainard, William A.; and Buckley, Donald H.: Scanning Electron Microscope Study of Polytetrafluoroethylene Sliding on Aluminum Single Crystals. NASA TN D-7321, 1973.

3. Brainard, William A.; and Buckley, Donald H.: Adhesion, Friction, and Wear of a Copper Bicrystal With (111) and (210) Grains. NASA TN D-7232, 1973.

4. Skinner, J.; Gane, N.; and Tabor, D.: Micro-friction of Graphite. Nature Physical Science, vol. 232, no. 35, Aug. 30, 1971, pp. 195-196.

5. Thornton, P.R.: Scanning Electron Microscopy. Chapman and Hall Limited, 1968.

6. Tegart, William, J.M.: Elements of Mechanical Metallurgy. Macmillian Company, 1966.

7. Avner, Sidney H.: Introduction to Physical Metallurgy. McGraw-Hill, 1964.

8. Smithells, Colin J., ed.: Metals Reference Book. Vol. III, 4th ed., Plenum Press, 1967.

9. Metals Handbook. The American Society for Metals, 1948.

TABLE I. - MECHANICAL PROPERTIES

	Elastic modulus, kg/mm^2 (a)	Shear modulus, kg/mm^2 (a)	Poisson's ratio (a)	Hardness (annealed Brinall), kg/mm^2	Hardness (20 percent cold worked), kg/mm^2	Recrystallization temperature, ^oC (b)
Aluminum	7.19×10^3	2.72×10^3	0.34	[c]15	[c, d]30	80
Copper	12.5	4.64	.34	[c]42	[c]96	110
Iron	21.7	8.47	.28	[e]75	[e]130	400

[a]Data from ref. 6.
[b]Data from ref. 7.
[c]Data from ref. 8.
[d]Fully hard.
[e]Data from ref. 9.

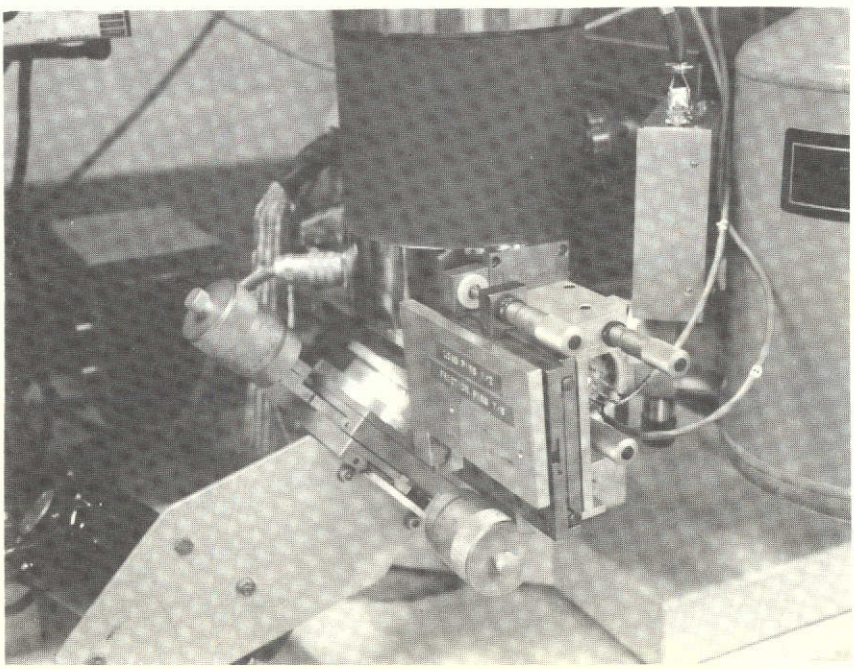

Figure 1. - Photograph of friction apparatus mounted on scanning electron microscope.

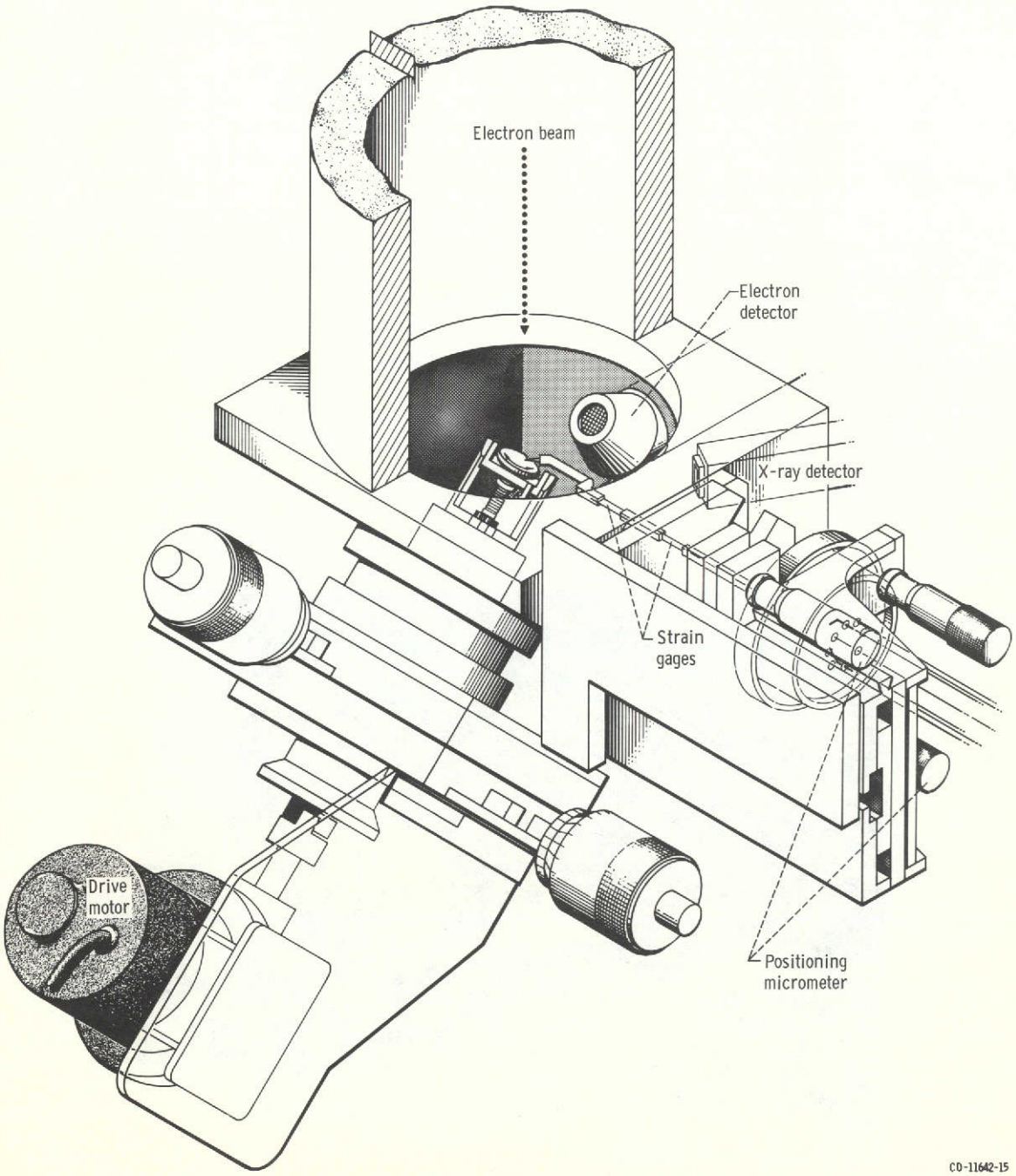

Figure 2. - Detailed drawing of friction apparatus mounted on scanning electron microscope.

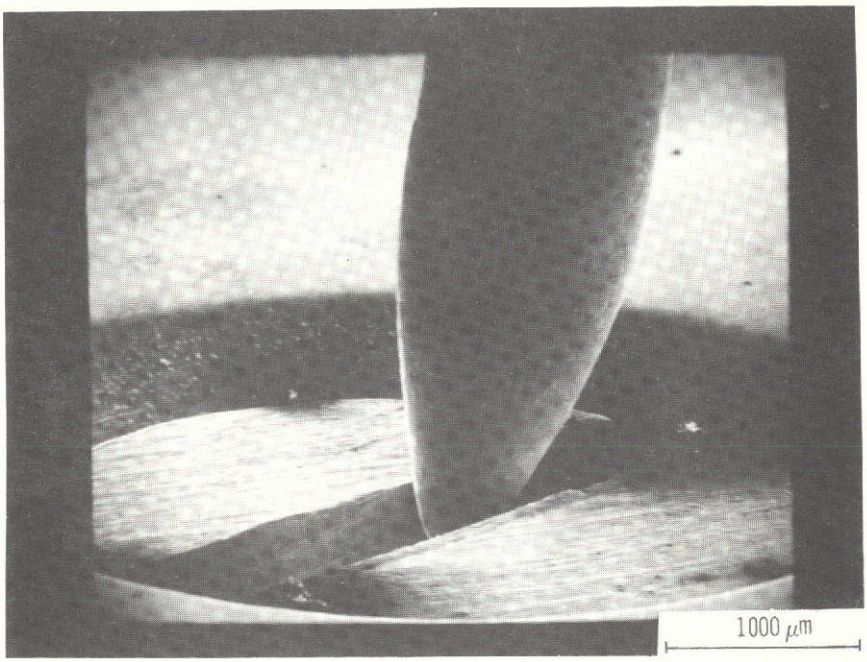

Figure 3. - Image showing rider specimen in center slot of screw holding disk to shaft.

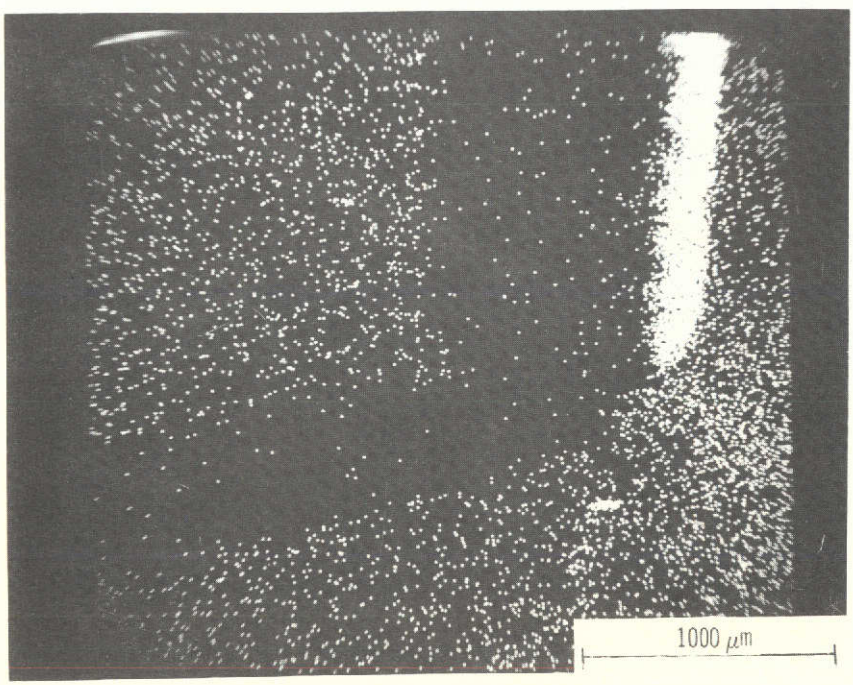

Figure 4. - X-ray map showing areas blocked from detector. X35.

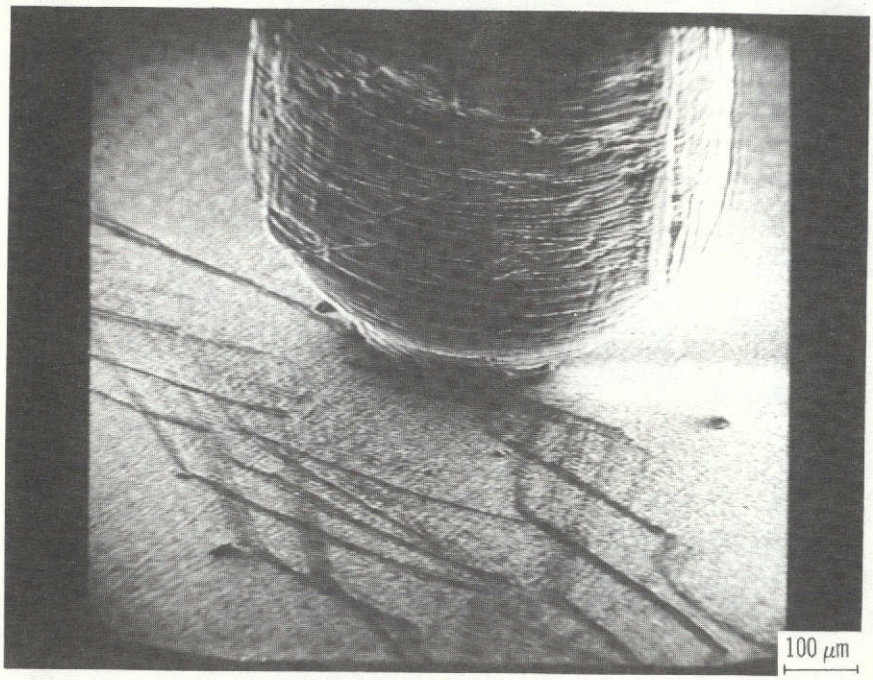

(a) Stick-slip wear track for aluminum sliding on aluminum. X100.

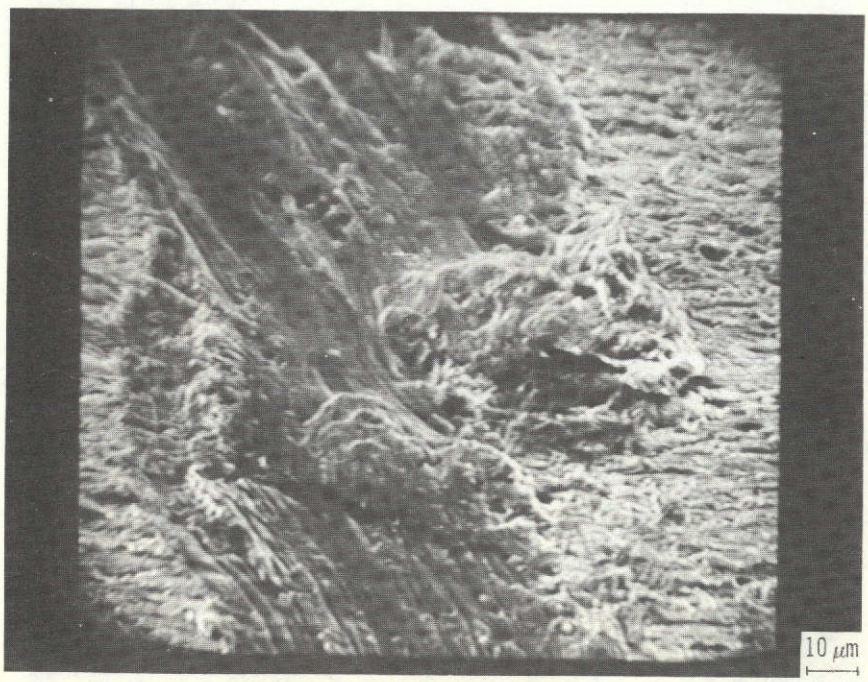

(b) Enlarged view of stick-slip furrow after slip. X700.

Figure 5. - Wear process for aluminum sliding on aluminum.

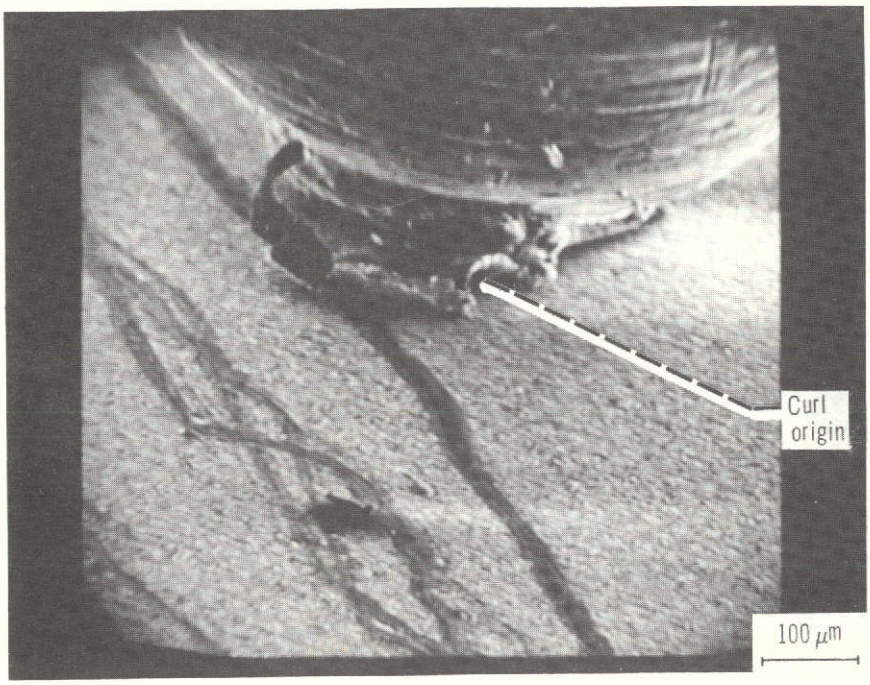

(a) Prow view.

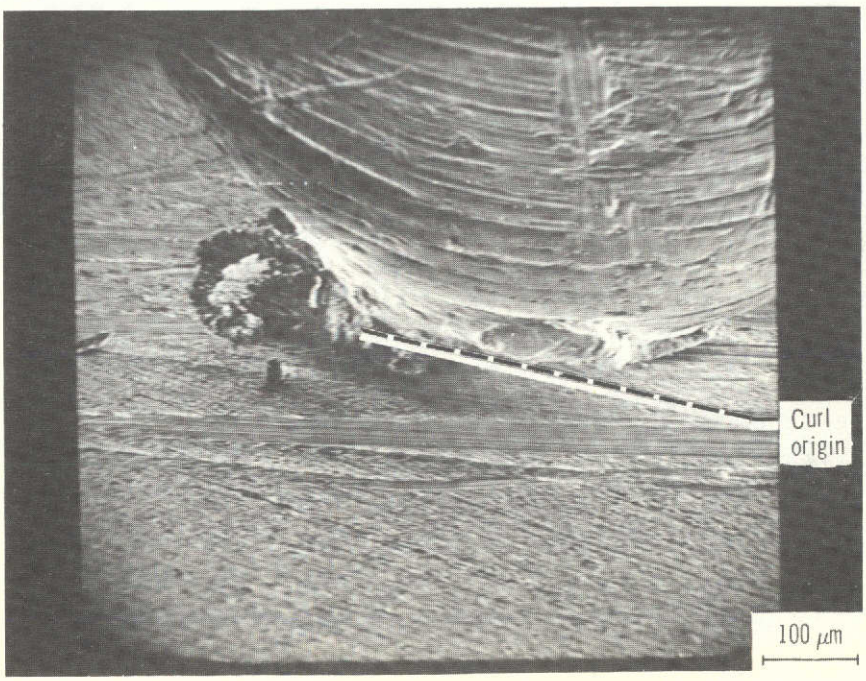

(b) Side view.

Figure 6. - Shearing of aluminum disk surface by abrasive aluminum prow.

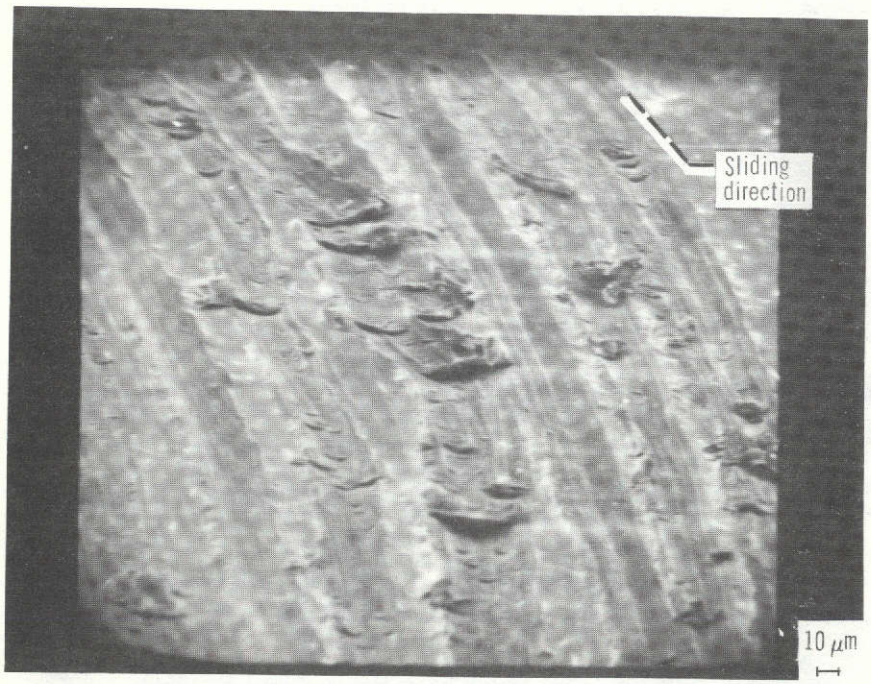

(a) Iron disk wear track.

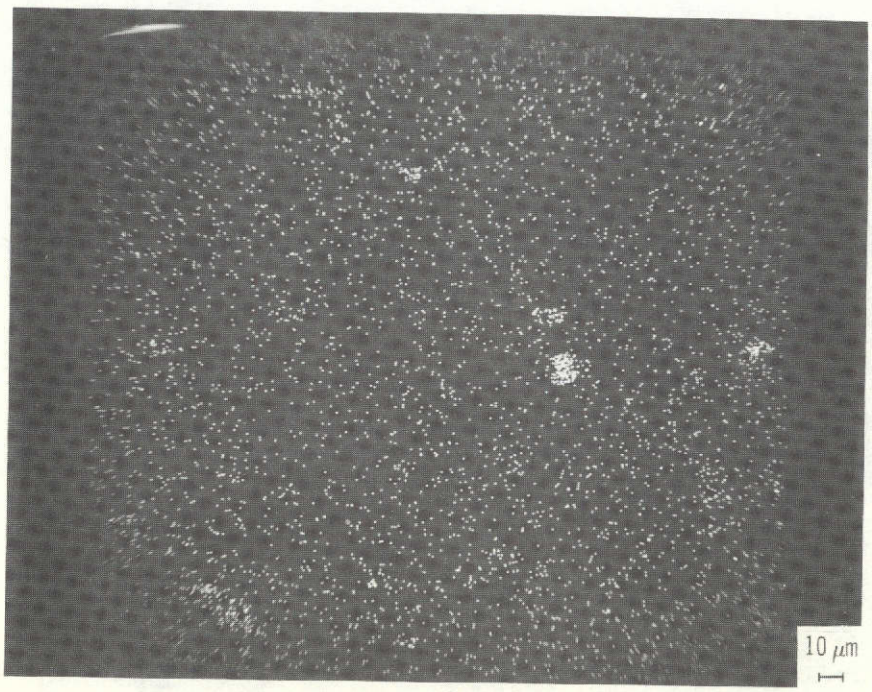

(b) Aluminum K_α X-ray map of iron disk wear track; 8000 counts.

Figure 7. - Wear track of iron disk after running with aluminum rider. X350.

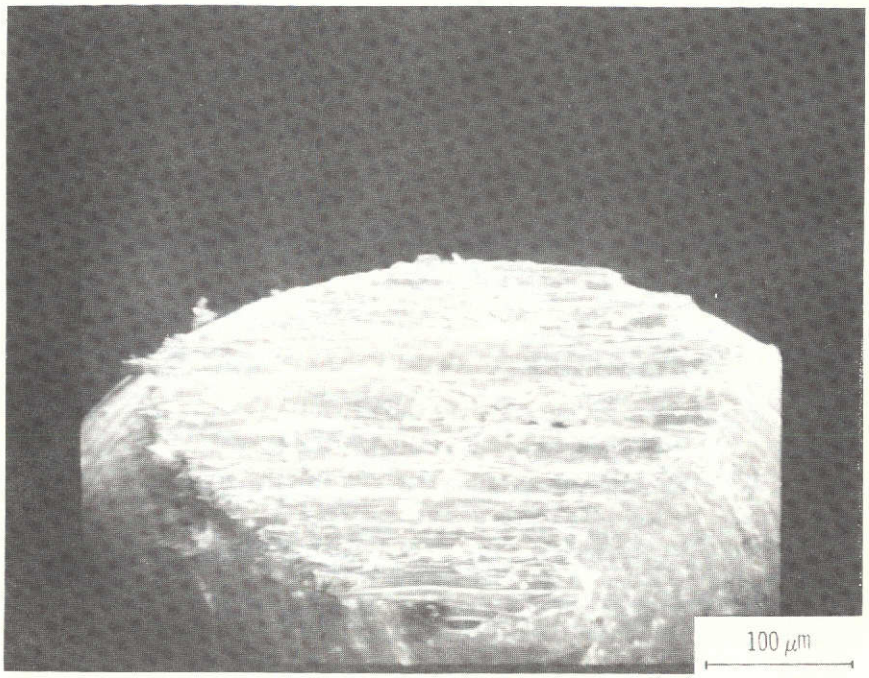

(a) Electron image of copper rider wear scar.

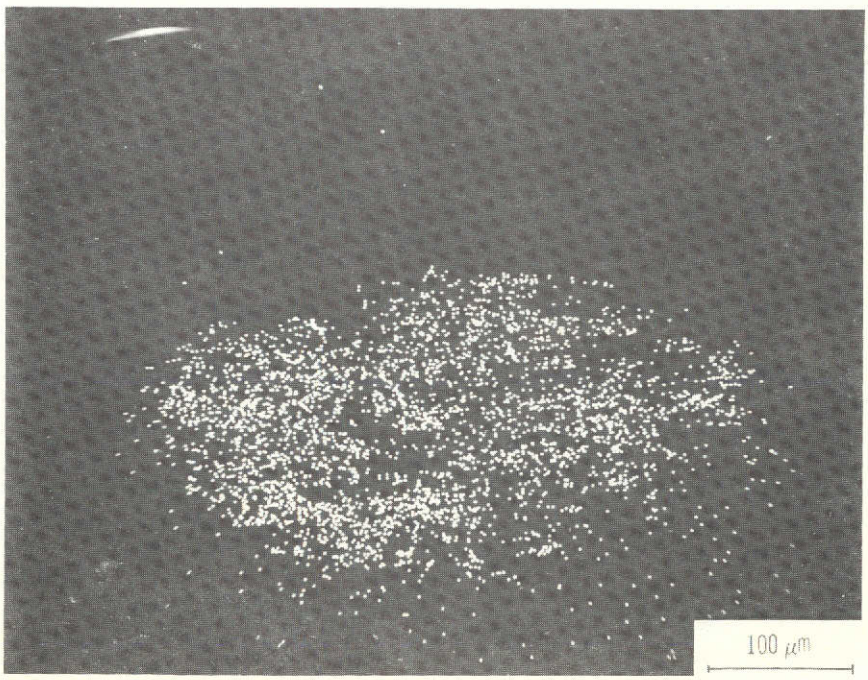

(b) Iron K_α map of aluminum rider; 4000 counts.

Figure 8. - Rider wear scar of aluminum rider after running on iron disk. X175.

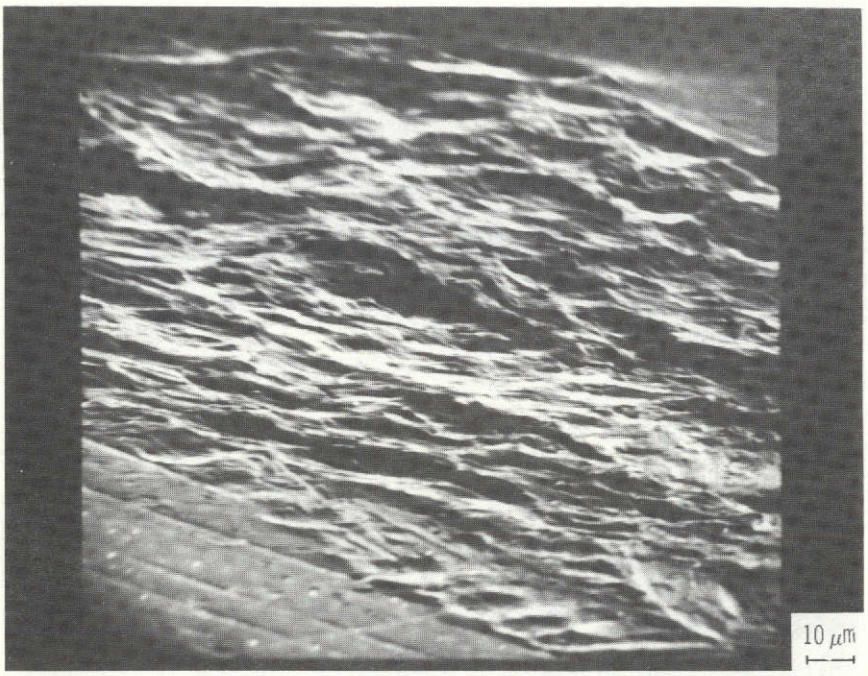

(a) Electron image.

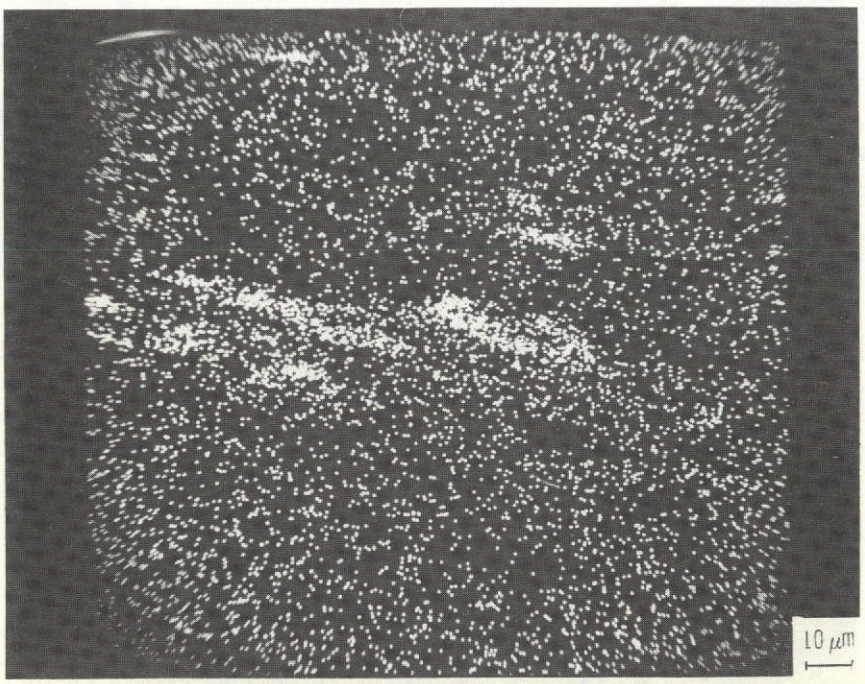

(b) Aluminum K_α X-ray map of copper disk wear track; 10 000 counts.

Figure 9. - Wear track of copper disk after running with aluminum rider. X700.

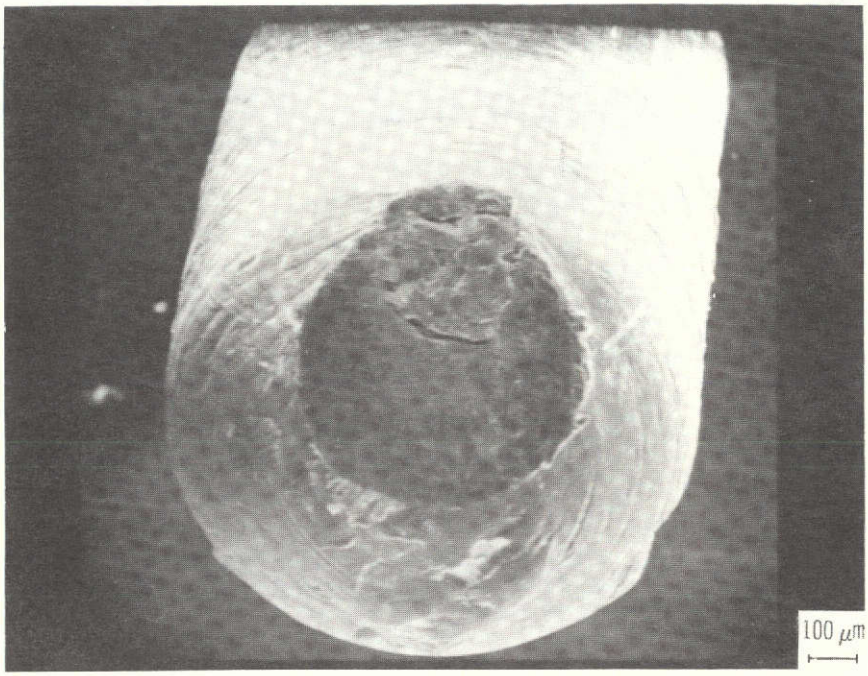

(a) Aluminum rider.

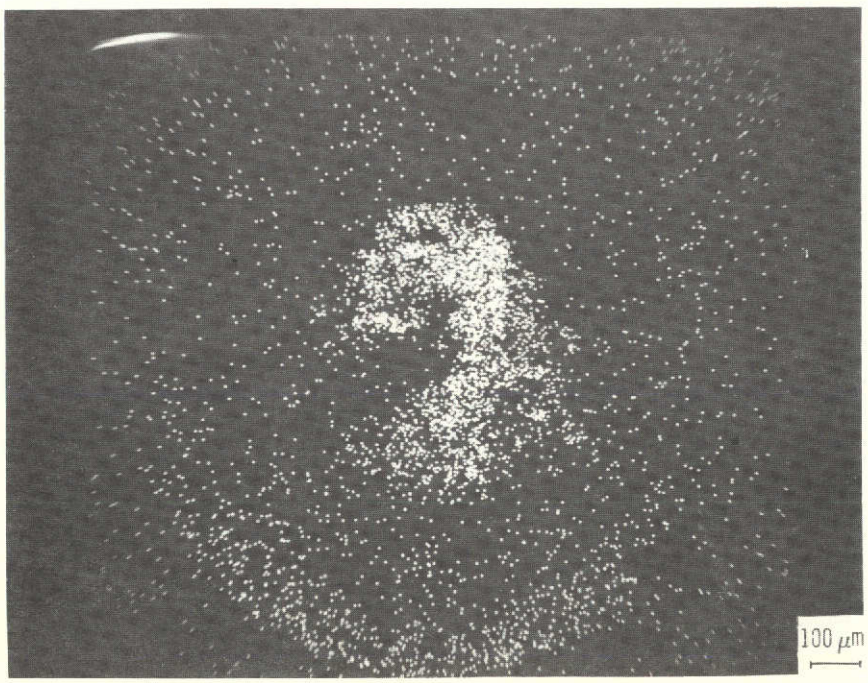

(b) Copper K_α X-ray map of aluminum rider; 15 000 counts.

Figure 10. - Rider wear scar of aluminum rider after running on copper disk. X700.

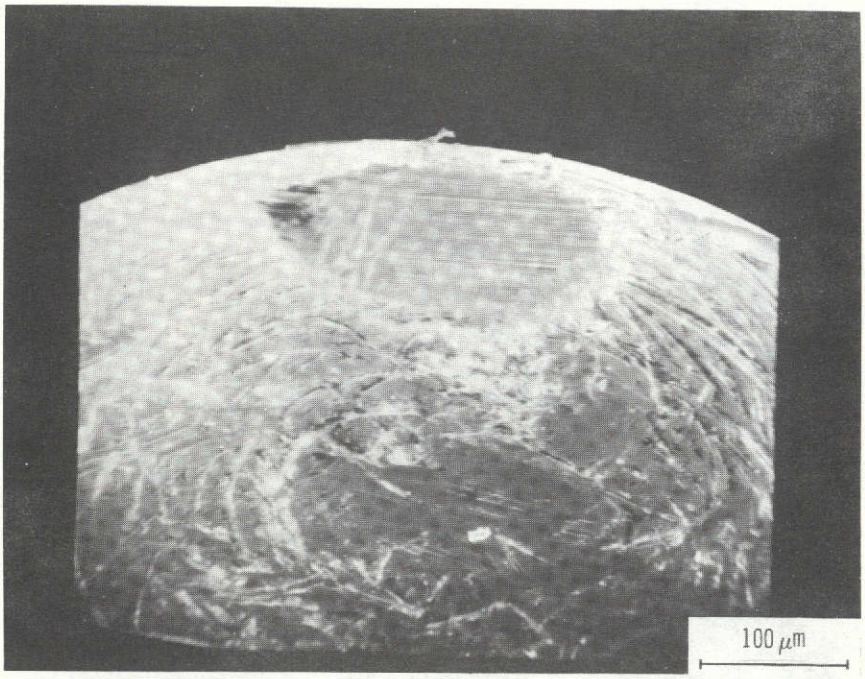

(a) Electron image of aluminum rider wear scar.

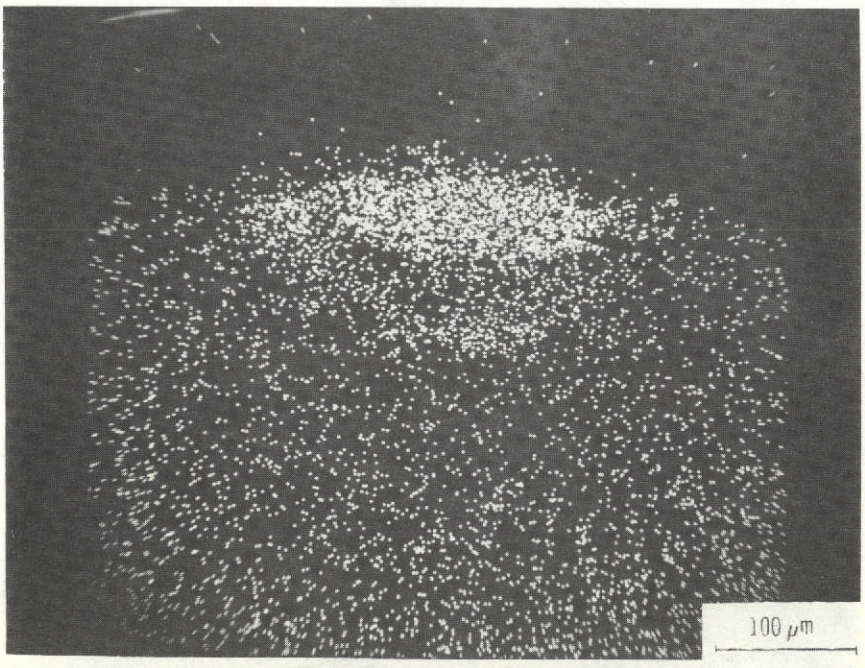

(b) Iron K_α X-ray map of copper rider wear scar; 8000 counts.

Figure 11. - Rider wear scar of copper rider after sliding on iron disk. X210.

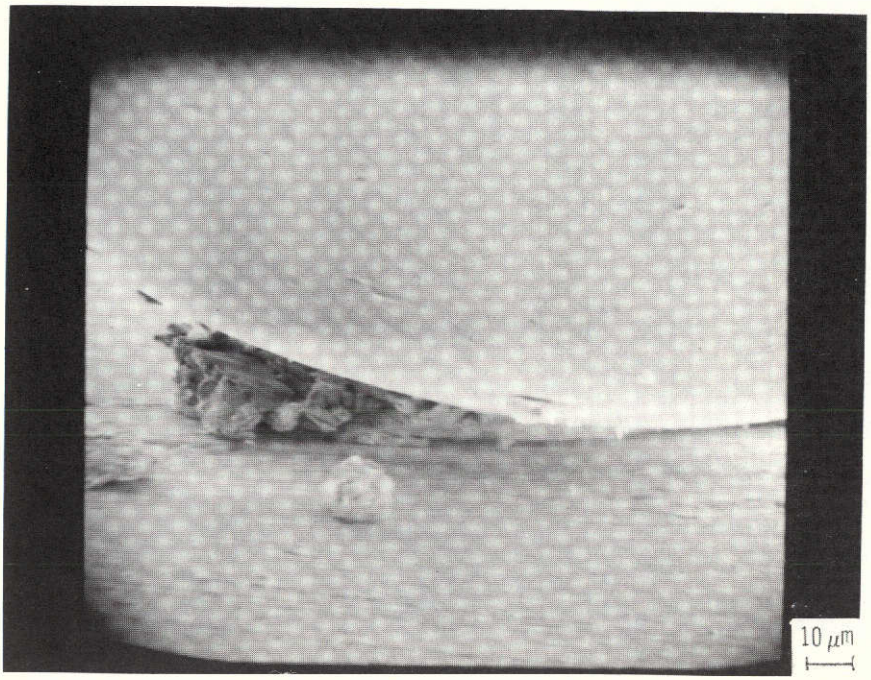

(a) Side view of wear process for iron sliding on copper. X350.

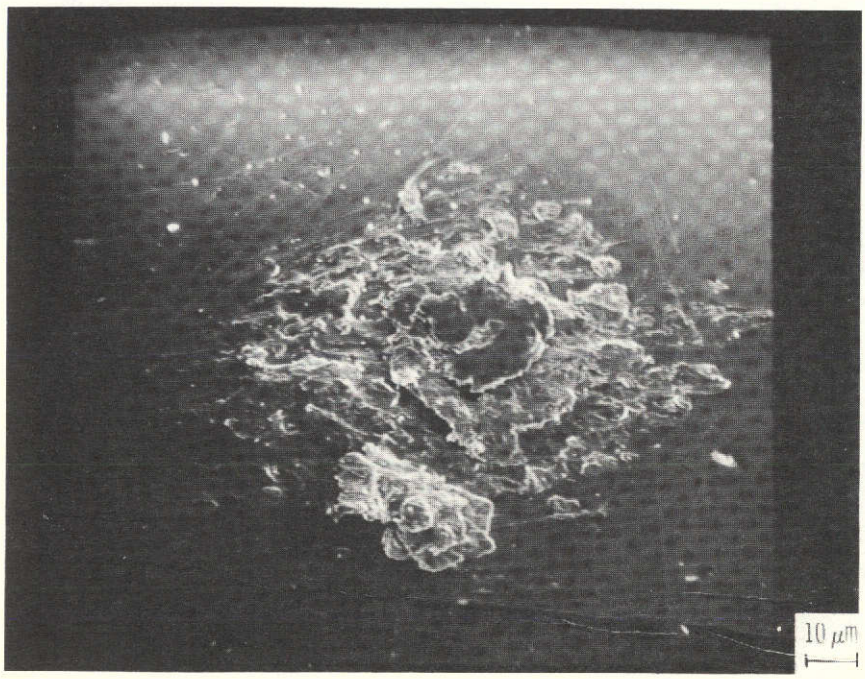

(b) Copper wear debris adhering to iron rider after sliding. X400.

Figure 12. - Results of iron sliding on copper.

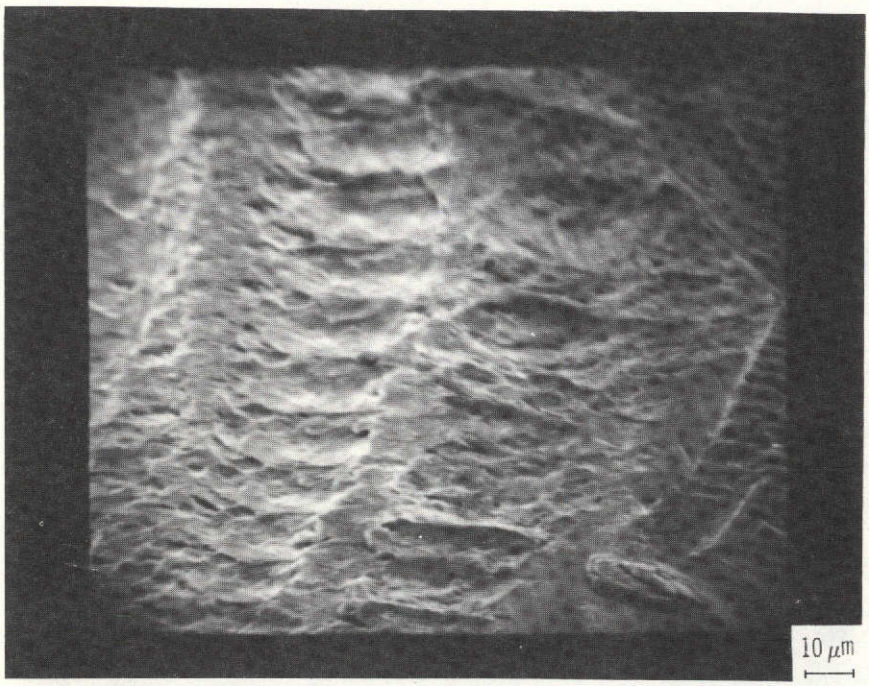

(a) Stick-slip.

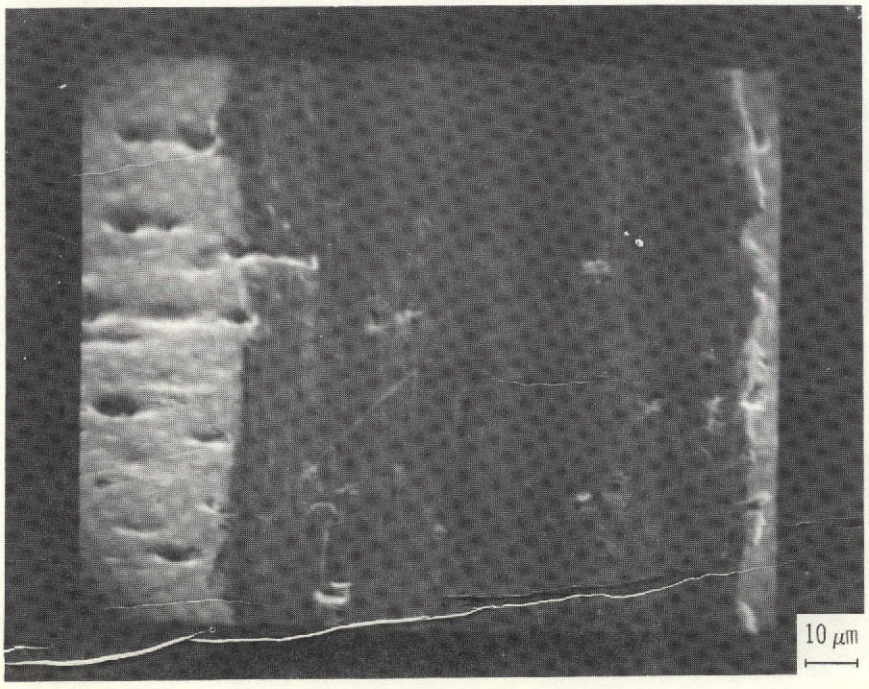

(b) Restrained from slip-stick.

Figure 13. - Aluminum wear tracks after sliding with iron rider. X600.

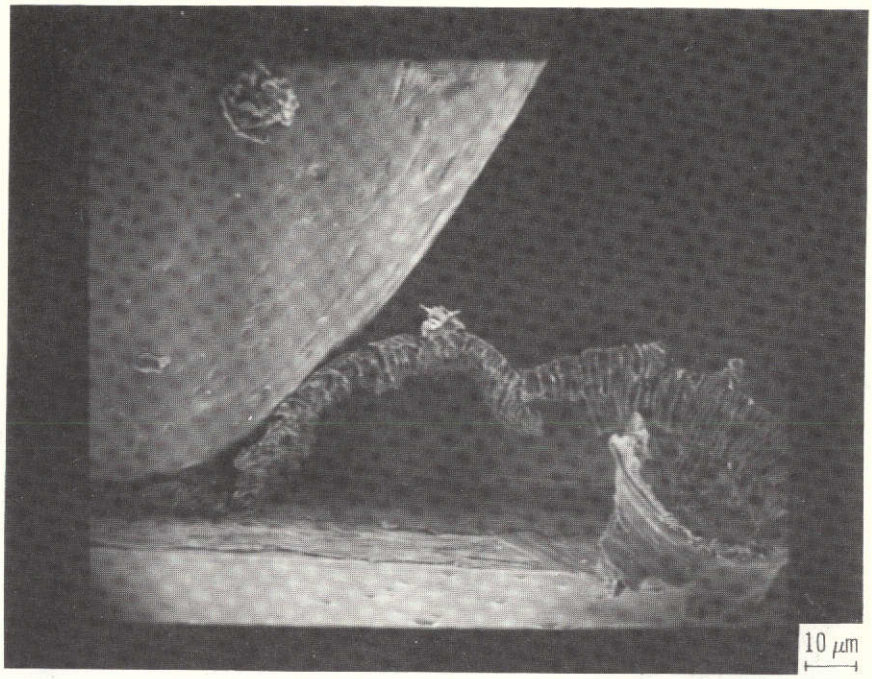

(a) X300.

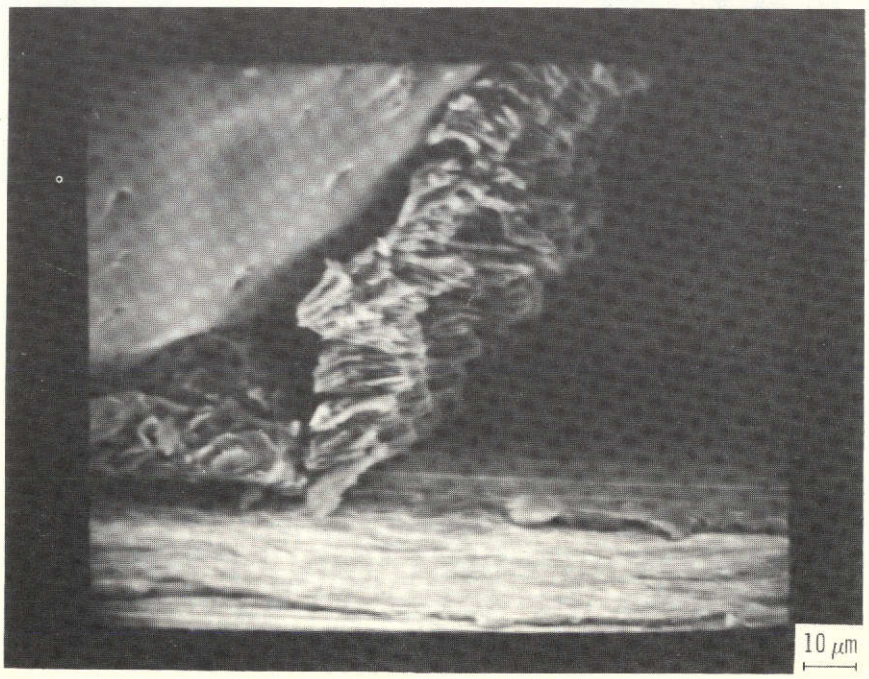

(b) X600.

Figure 14. - Machining of aluminum by iron rider in restrained mode.

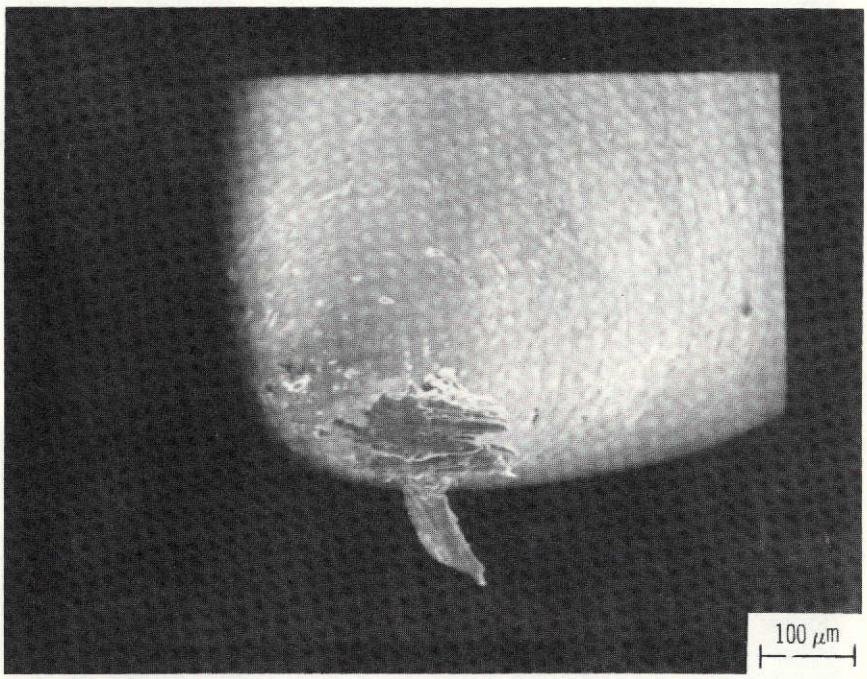

Figure 15. - Iron rider after sliding on aluminum.

NASA-Langley, 1974 E-7913